Nonlinear intensity effects in a laser generating the three main standing waves

F. Bretenaker* and A. Le Floch
Laboratoire d'Electronique Quantique, Physique des Lasers, Université de Rennes I, F-35042 Rennes CEDEX, France
(Received 30 October 1990)

The resonance condition is used to describe theoretically the three main kinds of standing waves with $\mathbf{E}\perp\mathbf{B}$ (linear) and $\mathbf{E}\parallel\mathbf{B}$ (helicoidal and circular polarizations) that can be produced by the same laser and their nonlinear interaction with an atomic medium. It is shown that the saturation behavior of a single-mode gas laser is drastically modified by the nature of the operating standing wave. The predictions are checked experimentally with a laser from which each kind of standing wave can be generated with the same losses. The anisotropic structure of the saturation and in particular of the Lamb dip is isolated in each case. Very good agreement is observed between experiments and theory.

I. INTRODUCTION

Renewed interest in the study of electromagnetic standing waves arose after Chu and Okhawa noticed that standing waves with parallel electric and magnetic fields can exist in free space.[1] This discovery led to many comments and much controversy.[2–8] Finally, the general conditions for the existence of transverse electromagnetic waves with $\mathbf{E}\parallel\mathbf{B}$ have been derived .[9–12] This discussion has led to a better knowledge of the different standing waves that can be produced by the superposition of different circularly polarized beams propagating in two opposite directions. The question one may ask now is how atoms behave in such standing waves. To answer this question, one may simply observe the behavior of a gas laser when the nature of the standing wave that is amplified by the atoms is changed. For simplicity, we shall reduce our study to the case of standing waves that are generated by different combinations of circularly polarized beams of equal amplitudes. This leads to only three types of standing waves, namely, the usual linearly, helicoidally, and circularly polarized standing waves. The case of elliptically polarized standing waves could also be considered, but this is a derivative and would not involve physics other than exhibited by these three standing waves. What is the nature of the observable effects one can expect from such an experiment? As these standing waves are all linear combinations of circularly polarized waves, the linear effects, i.e., gain and losses, will not be affected by the nature of the standing wave, as long as no external magnetic field is applied on the atoms, i.e., as long as the symmetry between the σ^+ and σ^- beams is not broken. We shall consequently focus our attention on nonlinear effects that occur in usual lasers, i.e., saturation effects. Some effects related to the cancellation of spatial-hole-burning-induced population modulation in Fabry-Pérot cavities with helicoidally polarized standing waves have already been discussed for giving single-mode characteristics to a solid-state laser.[13,14] Our discussion is restricted to single-mode lasers and the related spectral hole-burning effects. The organization of this paper is as follows. In Sec. II we present our notations and conventions for circularly polarized light and we derive the three considered standing waves. In Sec. III we describe the theoretical laser cavity used to produce successively these three standing waves without altering the cavity losses so as to be able to compare the different laser responses. We then derive the output power of the laser in each case using the resonance condition[15] and calculate the polarization of the medium up to third order in field.[16] Section IV is devoted to experiments. The predictions of Sec. III are checked with a He-Ne laser oscillating at 3.39 μm and the observation of the evolution of the output power when an axial magnetic field is applied to the atomic medium allows us to discuss physically the role of populations, Zeeman coherences, and orientation terms.

II. CONVENTIONS AND DESCRIPTION OF STANDING WAVES

Let us consider a set of unit vectors $\hat{\mathbf{x}}$, $\hat{\mathbf{y}}$, and $\hat{\mathbf{z}}$. For the description of circularly polarized waves in free space, we use the following convention: a traveling wave is said to be right-handed circularly polarized if an observer sees the electric field associated with the wave rotating in the clockwise direction when looking in the direction of propagation. This means that the electric fields $\mathbf{E}_r^+$ and $\mathbf{E}_l^+$ associated with the right- and left-handed circularly polarized traveling waves propagating in the $+z$ direction are given by

$$\mathbf{E}_r^+ = \mathcal{E}(\hat{\mathbf{x}} - i\hat{\mathbf{y}})\exp[i(\omega t - kz)] + \text{c.c.} , \quad (1)$$

$$\mathbf{E}_l^+ = \mathcal{E}(\hat{\mathbf{x}} + i\hat{\mathbf{y}})\exp[i(\omega t - kz)] + \text{c.c.} , \quad (2)$$

where $\mathcal{E}$ is the (real) field amplitude, ω the pulsation, and k the wave number. The corresponding right-handed and left-handed circularly polarized waves traveling in the $-z$ direction are given by

$$\mathbf{E}_r^- = \mathcal{E}(\hat{\mathbf{x}} + i\hat{\mathbf{y}})\exp[i(\omega t + kz)] + \text{c.c.} , \quad (3)$$

$$\mathbf{E}_l^- = \mathcal{E}(\hat{\mathbf{x}} - i\hat{\mathbf{y}})\exp[i(\omega t + kz)] + \text{c.c.} , \quad (4)$$

To define what we call σ^+ and σ^- waves, we must choose a reference oriented axis. This axis is usually chosen to be that of an external static magnetic field. Let us choose the $+z$ axis. Then the waves associated with $\mathbf{E}_r^+$ and $\mathbf{E}_l^-$ are said to be σ^+ waves and the waves associated with $\mathbf{E}_r^-$ and $\mathbf{E}_l^+$ and σ^- waves. One must notice that the concepts of right- and left-handed circular polarizations depend on the direction of propagation though the σ^+ and σ^- concepts depend only on the absolute direction of rotation of the electric field associated with the wave.

Let us now describe the three possible standing waves one can obtain with a superposition of such circularly polarized traveling waves of equal amplitude $\mathcal{E}$. The most common case is that of the x-linearly-polarized standing wave that is the sum of the four fields of Eq. (1)–(4):

$$\mathbf{E}_x = 8\mathcal{E}\hat{\mathbf{x}}\cos(\omega t)\cos(kz) \ . \tag{5}$$

The associated magnetic field $\mathbf{B}$ is given by the Maxwell-Faraday law [in Système International (SI) units] $\nabla\times\mathbf{E} = -\partial\mathbf{B}/\partial t$:

$$\mathbf{B}_x = 8\frac{\mathcal{E}}{c}\hat{\mathbf{y}}\sin(\omega t)\sin(kz) \ . \tag{6}$$

The usual electric and magnetic field distributions of this standing wave are shown in Fig. 1. This wave has the usual property $\mathbf{E}\perp\mathbf{B}$ and exhibits nodes and antinodes. The electric and magnetic fields are in quadrature, spatially as well as temporally.

The second standing wave considered here is the helicoidally polarized standing wave, first discussed independently by Evtuhov and Siegman,[13] and by Kastler.[17] The right-handed helicoidally polarized standing wave is the superposition of two counterpropagating right-handed circularly polarized traveling waves, i.e., a σ^+ wave propagating in the $+z$ direction and a σ^- wave propagating in the $-z$ direction. Its electric field $\mathbf{E}_h$ and magnetic field $\mathbf{B}_h$ are given by

$$\mathbf{E}_h = 4\mathcal{E}\cos(\omega t)[\hat{\mathbf{x}}\cos(kz) - \hat{\mathbf{y}}\sin(kz)] \ , \tag{7}$$

$$\mathbf{B}_h = -4\frac{\mathcal{E}}{c}\sin(\omega t)[\hat{\mathbf{x}}\cos(kz) - \hat{\mathbf{y}}\sin(kz)] \ . \tag{8}$$

The electric field distribution of such a wave is shown in Fig. 2. The electric field is distributed along a spatially constant amplitude helix. The whole helix oscillates in time at pulsation ω. Notice that this wave exhibits no nodes, as pointed out in Ref. 13 and 17, and has the property $\mathbf{E}\|\mathbf{B}$. This kind of standing wave is the one discussed by Chu and Okhawa in their paper dealing with $\mathbf{E}\|\mathbf{B}$ standing waves.[1]

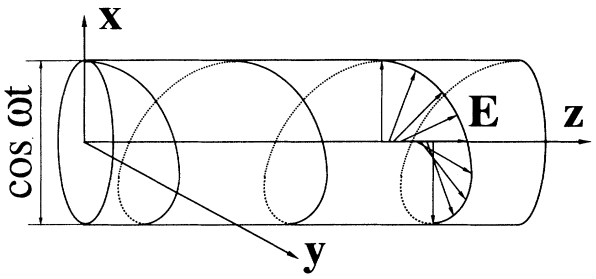

FIG. 2. Electric field distribution of a helicoidally polarized standing wave. The magnetic field $\mathbf{B}$ (not shown) is parallel to $\mathbf{E}$ and oscillates in time in quadrature with $\mathbf{E}$.

The third standing wave we discuss here is the circularly polarized standing wave, which is the superposition of, for example, two counterpropagating σ^+ waves, i.e., a right-handed circularly polarized traveling wave propagating in the $+z$ direction and a left-handed circularly polarized traveling wave propagating in the $-z$ direction. The associated electric and magnetic fields are given by

$$\mathbf{E}_c = 4\mathcal{E}\cos(kz)[\hat{\mathbf{x}}\cos(\omega t) + \hat{\mathbf{y}}\sin(\omega t)] \ , \tag{9}$$

$$\mathbf{B}_c = 4\frac{\mathcal{E}}{c}\sin(kz)[\hat{\mathbf{x}}\cos(\omega t) + \hat{\mathbf{y}}\sin(\omega t)] \ . \tag{10}$$

The field distributions of such a wave are shown in Fig. 3. One must notice that $\mathbf{E}_c$ and $\mathbf{B}_c$ are in the same plane in the whole space and that this plane oscillates in time at pulsation ω. This standing wave exhibits nodes and antinodes. This kind of $\mathbf{E}\|\mathbf{B}$ standing wave is the one discussed by Zaghloul, Volk, and Buckmaster.[9]

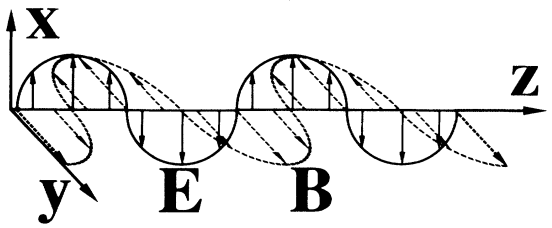

FIG. 1. Electric (solid line) and magnetic (dashed line) field distributions of a linearly polarized standing wave.

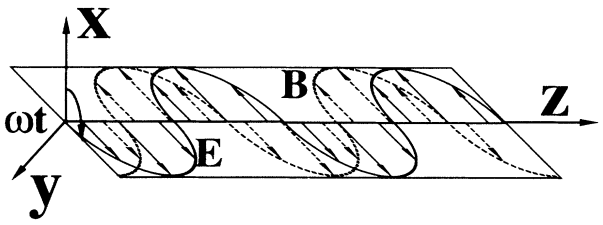

FIG. 3. Electric (solid line) and magnetic (dashed line) field distributions of a circularly polarized standing wave. Notice that here $\mathbf{E}$ is also parallel to $\mathbf{B}$.

III. THEORETICAL PREDICTIONS

As already stated in the Introduction, a convenient means of studying the behavior of atoms in these three different standing waves is to build a laser cavity where these three field distributions can be attained successively with the same losses. Such a cavity is shown schematically in Fig. 4. This cavity contains a Brewster plate P, a Faraday rotator FR providing a nonreciprocal polarization rotation ϕ depending on the applied magnetic field, and two quarter-wave plates QWP1 and QWP2 whose axes make angles ρ_1 and ρ_2 with respect to the x axis. The second quarter-wave plate has two possible positions, labeled 1 and 2. When QWP2 is in position 2 and $\phi=\rho_1=\rho_2=0$, the polarization is linear in the whole cavity and the active medium is submitted to a linearly polarized standing wave described by Eqs. (5) and (6). Let us now turn the first quarter-wave plate so that $\rho_1=45°$. The field distribution between the quarter-wave plates is now helicoidally polarized and the eigenfrequency can be changed by a rotation of QWP2.[13,15,18] If QWP2 is now placed in position 1 with $\phi=\rho_1=45°$ and $\rho_2=0°$, the field distribution between QWP2 and mirror M_2 is a circularly polarized standing wave, as suggested in Ref. 18 and realized by Kozin, Petrov, and Protsenko.[19] In this case, QWP1 is not necessary to create the circular standing wave but we keep it inside the cavity to keep constant losses. Notice that the scheme proposed by Bodlaj[20] using only a quarter-wave plate does not lead to such a circularly polarized standing wave. Besides, any elliptically polarized standing wave may be realized with other values of ρ_1 and ρ_2.[21]

We hence have a cavity in which the active medium can successively support propagation of the three considered standing waves. The expression of the output power can be obtained from the resonance condition[15] in the three different cases, as already obtained for the linearly and helicoidally polarized standing waves in Ref. 22. The resonance condition is written as

$$P_2R_2P_1R_1\mathbf{E}=\mathbf{E}\ , \tag{11}$$

where

$$R_1=\begin{bmatrix} r_x & 0 \\ 0 & r_y \end{bmatrix},\quad R_2=r\begin{bmatrix} 1 & 0 \\ 0 & 1 \end{bmatrix}$$

are the Jones reflection matrices, where r_x, r_y, and r are the reflection coefficients. P_1 and P_2 are the Jones propagation matrices in the active medium that have been calculated in Ref. 16. These matrices are obtained from a third-order development of the atomic medium polarization and are functions of the field amplitude. They extend to the case of nonlinear media the definition of the propagation matrix given by Jones for linear crystals.[23] The search of the eigenvalues in the resonance condition (11) using the expressions of P_1 and P_2 given in Ref. 16 then leads to the following expressions for the intensities of the linearly (I_x), helicoidally (I_h), and circularly (I_c) polarized standing waves:

$$I_x=\left[\frac{1}{L}\ln\frac{1}{rr_x}-\frac{2\omega N_0 S}{\epsilon_0 c\hbar k v_m}Z^i(\xi)\right]\times\left[\frac{2\omega N_0}{\epsilon_0\hbar c}[\mathrm{Re}(I_1+I_2)]\times\left[\frac{S_1+S_3}{\Gamma'_a(0)}+\frac{S_1+S_2}{\Gamma'_b(0)}+\frac{S_2}{\Gamma'_a(2)}+\frac{S_3}{\Gamma'_b(2)}\right]\right]^{-1}, \tag{12}$$

$$I_h=\left[\frac{1}{L}\ln\frac{1}{rr_x}-\frac{2\omega N_0 S}{\epsilon_0 c\hbar k v_m}Z^i(\xi)\right]\times\left\{\frac{2\omega N_0}{\epsilon_0\hbar c}\left[2\,\mathrm{Re}I_1\left[\frac{S_1}{\Gamma'_a(0)}+\frac{S_1}{\Gamma'_b(0)}\right]+2\,\mathrm{Re}I_2\left[\frac{S_2}{\Gamma'_b(0)}+\frac{S_3}{\Gamma'_a(0)}\right]\right]\right\}^{-1}, \tag{13}$$

$$I_c=\left[\frac{1}{L}\ln\frac{1}{rr_x}-\frac{2\omega N_0 S}{\epsilon_0 c\hbar k v_m}Z^i(\xi)\right]\times\left[\frac{2\omega N_0}{\epsilon_0\hbar c}2[\mathrm{Re}(I_1+I_2)]\left[\frac{S_1}{\Gamma'_a(0)}+\frac{S_1}{\Gamma'_b(0)}\right]\right]^{-1}, \tag{14}$$

where L is the cavity length, ϵ_0 is the vacuum permittivity, $Z(\xi)$ is the plasma dispersion function[24] with $\xi=(\omega-\omega_{ab})/(kv_m)+i\Gamma'_{ab}/kv_m=x+iy$, N_0 is the excitation parameter, kv_m is the Doppler width of the medium, Γ'_{ab} is the relaxation rate of optical coherences ($\Delta m=\pm1$ processes), $\Gamma'_{a,b}(0)$ and $\Gamma'_{a,b}(2)$ are the relaxation rates of the level populations ($\Delta m=0$ processes) and Zeeman coherences ($\Delta m=\pm2$ processes), respectively, and I_1 and I_2 are the usual velocity integrals[25] given by

$$I_1=\frac{1}{(\hbar k v_m)^2}\left[Z'(\xi)-\frac{1}{y}Z^i(\xi)\right],$$

$$I_2=\frac{1}{(\hbar k v_m)^2}\left[\frac{1}{x}Z^r(\xi)-\frac{1}{\xi}Z(\xi)\right].$$

S, S_1, S_2, and S_3 represent the following dipole matrix element sums:

$$S=\sum_m|\mu_{a_m b_{m\pm1}}|^2,\quad S_1=\sum_m|\mu_{a_m b_{m+1}}|^4,$$

$$S_2=\sum_m|\mu_{a_m b_{m+1}}|^2|\mu_{b_{m+1}a_{m+2}}|^2,$$

$$S_3=\sum_m|\mu_{a_m b_{m+1}}|^2|\mu_{a_m b_{m-1}}|^2.$$

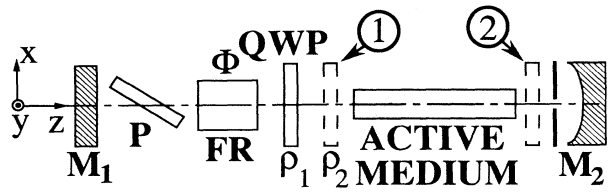

FIG. 4. Scheme of the laser cavity. The two mirror cavity (M_1,M_2) contains one Brewster plate P, a Faraday rotator FR, and two quarter-wave plates QWP. The second QWP has two possible positions, labeled 1 and 2.

Let us consider a $J_b=1\rightarrow J_a=2$ transition like the 3.39-μm He-Ne transition that will be used in experiments. In this case the preceding sums are proportional to the reduced matrix element with the values $S_1\sim 46$, $S_2\sim 21$, and $S_3\sim 1$. In the low-pressure approximation, the different relaxation rates $\Gamma'_{a,b}$ can be considered as equal.[26] Then Eqs. (12)–(14) can be written

$$I_x = A'[1-B'Z^i(\zeta)]/d_x \ , \tag{15}$$

$$I_h = A'[1-B'Z^i(\zeta)]/d_h \ , \tag{16}$$

$$I_c = A'[1-B'Z^i(\zeta)]/d_c \ , \tag{17}$$

where A' and B' describe the gain and losses of the laser. At line center and for the same excitation, the ratios of the denominators of (15)–(17) are

$$d_h/d_x=(2S_1+S_2+S_3)/2(S_1+S_2+S_3)\approx 0.84 \ , \tag{18}$$

$$d_c/d_x=4S_1/2(S_1+S_2+S_3)\approx 1.35 \ . \tag{19}$$

Moreover, the coefficients of the I_2 integral that describes the Lamb dip are in ratio

$$(S_2+S_3)/(S_1+S_2+S_3)\approx 0.32 \tag{20}$$

for the helicoidally and linearly polarized eigenstates and

$$2S_1/(S_1+S_2+S_3)\approx 1.35 \tag{21}$$

for the circularly and linearly polarized eigenstates. What is the physical meaning of these results? First, one can see from Eqs. (15)–(17) that the nature of the standing wave does not modify the *linear* behavior of the laser, i.e., the numerator of the output intensity expression. However, the *nonlinear* terms, i.e., the denominators d_x, d_h, and d_c, are greatly affected by the nature of the standing wave. On the one hand, the comparison between the linear and helicoidal cases shows, as already explained in Ref. 22, that the Lamb dip of the linearly polarized standing wave contains contributions due to both population effects and alignment effects. In the helicoidal Lamb dip, the former effects are present but the latter are not to be taken into account. Indeed, the helicoidally polarized standing wave is constructed from two different, counterpropagating σ waves that weakly interact and do not lead to a Zeeman coherence effect. On the other hand, let us compare the nonlinear behaviors of the linearly and circularly polarized eigenstates. As the circularly polarized standing wave contains two identical counterpropagating σ waves, it uses only half of the transitions between the Zeeman sublevels and leads to greater saturation effects than in the linear case, as seen from the ratio (19). Moreover, the two counterpropagating σ waves of the circularly polarized standing wave induce the same kind of orientation of the atoms. This explains why the Lamb dip must be so important in the case of the circularly polarized standing wave. In summary, we have predicted that, for a single-mode laser, three different Lamb dips correspond to each main standing wave. The strongest corresponds to the circularly polarized standing wave and the weakest one to the helicoidally polarized standing wave. These results highlight the different structures of the Lamb dip that will be explored experimentally. These structures will be confirmed by the study of the response of the laser to an axial magnetic field which will be shown to destroy some of the nonlinear contributions to the Lamb dip.

IV. EXPERIMENTAL RESULTS

The cavity is obtained as shown in Fig. 4 with mirror M_1 being plane and totally reflecting and mirror M_2 having a 1.2-m radius of curvature and transmitting 5% of the intensity. The cavity is 69 cm long and the discharge tube is 31 cm long and has a 3.5 mm inner diameter. The active medium that provides amplification at $\lambda=3.39$ μm is a ^{3}He-^{20}Ne 5:1 mixture at total pressure $P=0.5$ Torr. The Faraday rotator is a 15-mm-long gallium-doped yttrium iron garnet (Ga:YIG) crystal providing the needed 45° of rotation. The plane mirror is translated by a piezoelectric transducer in order to record the output power of the laser versus frequency. The results are shown for each kind of standing wave in Figs. 5(a)–5(c). As expected, the Lamb dip in the helicoidal case is much smaller than in the linear and circular cases and the output power is less important in the case of the circularly polarized standing wave. The comparison with theory can be performed with the following expression for the output power:

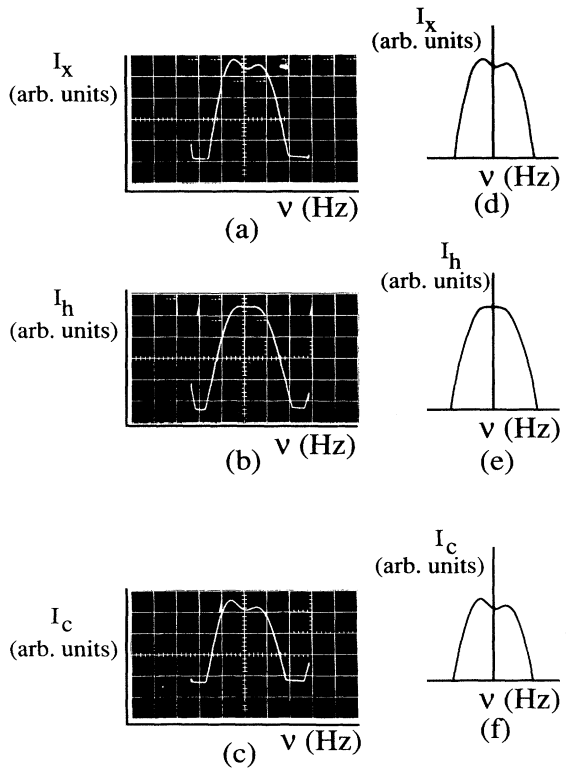

FIG. 5. Experimental (a)–(c) and theoretical (d)–(f) output power (in arbitrary units) vs frequency profiles in the case of the linearly [(a), (d)], helicoidally [(b), (e)], and circularly [(c), (f)] polarized standing waves (ν axis: 50 MHz per division, increasing from left to right).

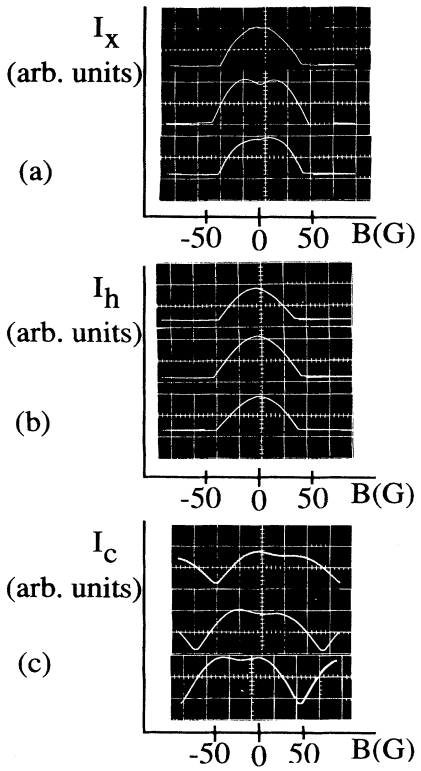

FIG. 6. Experimental output power vs axial magnetic field profiles in the case of the (a) linearly, (b) helicoidally, and (c) circularly polarized standing waves. The profiles are shown for three detunings in each case (-30, 0, $+30$ MHz).

$$I(v)=A\left\{1-B(v)\exp\left[\left[\frac{\omega-\omega_{ab}}{kv_m}\right]^2\right]\right\}\times\left[1+\frac{D\gamma^2}{\gamma^2+(\omega-\omega_{ab})^2}\right]^{-1}, \quad (22)$$

where γ is the homogeneous linewidth, B is the loss parameter that takes frequency-dependent losses into account and describes the output power profile asymmetries,[27] A is a scale factor, and D is the Lamb dip enhancement factor. The theoretical fits of Fig. 5(d)–5(f) have been obtained with Eq. (22), $kv_m=2\pi\times175$ MHz and $\gamma=2\pi\times30$ MHz and $A_x=50.8$ and $D_x=0.45$ in the case of the linearly polarized standing wave, $A_h=44$ and $D_h=0.13$ in the case of the helicoidally polarized standing wave, and $A_c=40.5$ and $D_c=0.55$ in the case of the circularly polarized standing wave. These results lead to the following ratios:

$$d_h/d_x=[(1+D_h)/A_h][(1+D_x)/A_x]^{-1}\approx0.90\ ,$$
$$d_c/d_x=[(1+D_c)/A_c][(1+D_x)/A_x]^{-1}\approx1.34$$

in agreement with (18) and (19). The experimental ratios for the Lamb dip are

$$D_h/D_x\approx0.29\ ,$$
$$D_c/D_x\approx1.22$$

in agreement with (20) and (21). Discussion of the role of populations, orientation, and Zeeman coherences in saturation effects can be made from the experimental results shown in Fig. 6. This figure displays the output power profiles versus axial magnetic field applied on the active medium, through use of a solenoid for three different detunings (0, ±30 MHz) for each kind of standing wave. The main effect of this magnetic field is to separate the center frequencies of the σ^+ and σ^- gain curves. This separation, which is about 1.58 MHz/G, leads indeed to a destruction of Zeeman coherences. In the case of the linearly polarized standing wave, the zero magnetic field resonance due to Zeeman coherences can consequently be observed at $B=0$ [Fig. 6(a)]. This resonance disappears in the case of the helicoidally polarized standing wave [Fig. 6(b)], because in this case the two counterpropagating traveling waves are of opposite σ and hence deal with different transitions. The case of the circularly polarized standing wave is very different from the preceding ones [Fig. 6(c)]. Indeed, in this case, the two counterpropagating traveling waves interact only with the σ^+ transitions. Consequently, the application of the axial magnetic field leads simply to a frequency shift of the gain curve, as can be seen from the photographs of Fig. 6(c). In this case, varying the magnetic field is almost equivalent to scanning the cavity frequency.

V. CONCLUSION

In conclusion, we have shown theoretically and experimentally that the three main standing waves either with $\mathbf{E}\perp\mathbf{B}$ (linear) or $\mathbf{E}\|\mathbf{B}$ (helicoidal and circular) are achievable in the same laser cavity and exhibit very different nonlinear interactions with an atomic medium. It has been proved that, as could be expected, the nontrivial relation $\mathbf{E}\|\mathbf{B}$ does not play any role in saturation effects. However, we have shown that the saturation terms in a single-mode gas laser are drastically modified by the nature of the standing wave and have different origins: isotropic population effects and anisotropic Zeeman coherences and orientation effects. Such a structure completes the usual Bennett hole picture of the Lamb dip introduced in the early years of laser physics.[28] It shows that the Lamb dip is not only due to population saturation effects, as usually stated.[29] On the contrary, the three different standing waves correspond to three different Lamb dips with their own particular structures. This discussion might be extended to other transitions with different values of the angular momenta of the levels where the differences between the effects might be even larger. The effects observed here in the case of gain saturation must of course have their equivalent in saturated absorption spectroscopy, inside or outside the laser cavity (inverse Lamb dip). Moreover, we have restrained here our discussion to the anisotropic contributions of the gain of the medium. The dispersion of the medium must certainly also deserve a similar discussion, leading to consequences in today's saturated absorption meterology.

ACKNOWLEDGMENTS

The Laboratoire d'Electronique Quantique is "associé au Centre National de la Recherche Scientifique No. 1202." The authors are happy to thank J. P. Taché for his helpful remarks. This research was partially supported by the "Direction des Recherches, Etudes et Techniques," the "pôle optique and optoélectronique de Formation des Ingénieurs par la Recherche Technologique," the "Centre Interuniversitaire de Calcul de Bretagne," and the "Etablissement Public Régional."

---

*Also at: Société d' Applications Générales d'Electricité et de Mécanique, Boîte Postale 72, 95101 Argenteuil CEDEX, France.

[1]C. Chu and T. Okhawa, Phys. Rev. Lett. **48**, 837 (1982).

[2]A. Khare and T. Pradhan, Phys. Rev. Lett. **49**, 1227 (1982); **49**, 1549 (1982); **51**, 1108 (1983).

[3]K. K. Lee, Phys. Rev. Lett. **50**, 138 (1983).

[4]C. Chu, Phys. Rev. Lett. **50**, 139 (1983).

[5]F. C. Michel, Phys. Rev. Lett. **52**, 1351 (1984).

[6]A. Khare and T. Pradhan, Phys. Rev. Lett. **52**, 1352 (1984).

[7]N. Salingaros, Am. J. Phys. **53**, 361 (1985); J. Phys. A **19**, L101 (1986); **19**, L705 (1986).

[8]K. R. Brownstein, J. Phys. A **19**, 159 (1986).

[9]H. Zaghloul, K. Volk, and H. A. Buckmaster, Phys. Rev. Lett. **58**, 423 (1987).

[10]C. Chu and T. Okhawa, Phys. Rev. Lett. **58**, 424 (1987).

[11]H. Zaghloul and H. A. Buckmaster, Am. J. Phys. **58**, 306 (1990).

[12]K. Shimoda, T. Kawai, and K. Uehara, Am. J. Phys. **58**, 394 (1990).

[13]V. Evtuhov and A. E. Seigman, Appl. Opt. **4**, 142 (1965).

[14]D. A. Dragert, IEEE J. Quantum Electron. **QE-8**, 235 (1972); D. J. De Jong and D. Andreou, Opt. Commun. **22**, 138 (1977).

[15]A. Le Floch and R. Le Naour, Phys. Rev. A **4**, 290 (1971); A. Le Floch and G. Stephan, *ibid.* **6**, 845 (1972); C. R. Acad. Sci. **277**, 265 (1973).

[16]G. Stephan, R. Le Naour, and A. Le Floch, Phys. Rev. A **17**, 733 (1978).

[17]A. Kastler, C. R. Acad. Sci. **271**, 999 (1970).

[18]A. Le Floch, Thése d'Etat, Université de Rennes, France, 1977 (unpublished).

[19]G. I. Kozin, V. V. Petrov, and E. D. Protsenko, Opt. Spektrosk. **62**, 1342 (1987) [Opt. Spectrosc. (USSR) **62**, 792 (1987)].

[20]V. Bodlaj, Opt. Commun. **6**, 12 (1972).

[21]R. Le Naour (private communication).

[22]A. Le Floch, R. Le Naour, and G. Stephan, Phys. Rev. Lett. **39**, 1611 (1977).

[23]R. C. Jones, J. Opt. Soc. Am. **38**, 671 (1948), and previous papers of the series.

[24]B. D. Fried and S. D. Conte, *The Plasma Dispersion Function* (Academic, New York, 1961).

[25]W. E. Lamb, Jr., Phys. Rev. **134**, A1429 (1964); M. Sargent III, M. O. Scully, and W. E. Lamb, Jr., *Laser Physics* (Addison-Wesley, Reading, MA, 1974); M. Sargent III and M. O. Scully, in *Laser Handbook*, edited by F. T. Arecchi and E. D. Schulz-Dubois (North-Holland, Amsterdam, 1972), Vol. 1, p. 45.

[26]M. Dumont, Thése d'Etat, Université de Paris, France, 1971 (unpublished); Phys. Rev. Lett. **28**, 1357 (1972).

[27]A. Le Floch, R. Le Naour, J. M. Lenormand, and J. P. Taché, Phys. Rev. Lett. **45**, 544 (1980); J. P. Taché, A. Le Floch, and R. Le Naour, Opt. Commun. **71**, 179 (1989).

[28]W. R. Bennett, Jr., Phys. Rev. **126**, 580 (1962).

[29]V. P. Chebotayev, in *Laser Handbook*, edited by M. Bass and M. L. Stitch (North-Holland, Amsterdam, 1985), Vol. 5, p. 289.